Entropy QC for Bayesian facies estimations

John V. Pendrel, Henk J. Schouten CGG*

Summary

We use the concepts of entropy and information theory to design a confidence measure for Bayesian facies estimations. Bayesian analyses provide the probabilities of occurrence of each constituent facies in a set. The entropy analysis uses all of these to establish a Confidence Index describing the reliability that the most-probable facies is in fact a clear best choice.

We apply these ideas to various facies estimates from Gulf of Mexico inversions. We demonstrate how entropy can be used to compare two different deterministic inversion workflows and measure the reliability of each. We also use the technique to QC the facies from simultaneous geostatistical inversion. Last, we demonstrate how Confidence Index templates can be used to predict the effectiveness of Bayesian facies estimation.

Introduction

Bayes' rule maps prior probabilities to posterior probabilities, given new information. In our present context, the probabilities are those of a set of facies which can be present within the reservoir. Prior information should generally be 3D in nature and can come from well logs or various geologic scenarios. The new information comes from the results of seismic inversions or their derivatives.

Facies can be described in elastic space using probability density functions (ePDFs) designed from elastic logs and rock physics models. Bayes' rule can then applied to the inversion results superimposed on those ePDFs. The process produces volumes of probabilities of occurrences of each of the facies in the set at all locations in 3D space (Pendrel et al., 2006).

We follow Pendrel and Schouten (2019) to find a confidence measure that incorporates the complete set of facies probabilities. When a single facies has a probability close to unity and the other possible facies have small probabilities, our confidence is clear. But when the competing facies are larger or, in the extreme, all facies have equal probability, what is the effect on confidence? We use the ideas of entropy and information theory to design a Confidence Index which can measure the reliability of different regions in the reservoir or compare the results of two different Bayesian-based workflows.

Method

We follow the work of Caulfield et al., 2018 and utilize the definition of entropy described by Shannon (1948). For a set of N facies with probabilities of occurrence, p_i, the entropy is

$$\mathrm{H} = -\sum_{i=1}^{N} p_i ln(p_i) \qquad \text{N = \# facies} \quad p_i = \text{probability of } i^{th} \text{ facies}$$

In the above equation, p_i is the Bayesian probability of occurrence of the i-th facies in the set of N.

When all the probabilities, p_i, are equal, the entropy is a maximum. Therefore,

$$\mathrm{H}_{\max} = -\ln\left(\frac{1}{N}\right)$$

When one of the facies is dominant and has a probability close to 1, the entropy will be near minimum. This will be our situation of most interest. We can create a confidence measure by computing a scaled negative entropy that takes on values in the range zero to unity. We refer to this measure as the Confidence Index (C.I.).

$$\text{C.I.} = 1 - \mathrm{H}/\mathrm{H}_{\max}$$

The Confidence Index is zero when all the probabilities are equal and unity when the probability of a single facies is 1. The behaviour of entropy for a set of three facies probabilities is further demonstrated in Figure 1. The green curve represents the case where $p_3 = 0$ and $p_1 + p_2 = 1$.

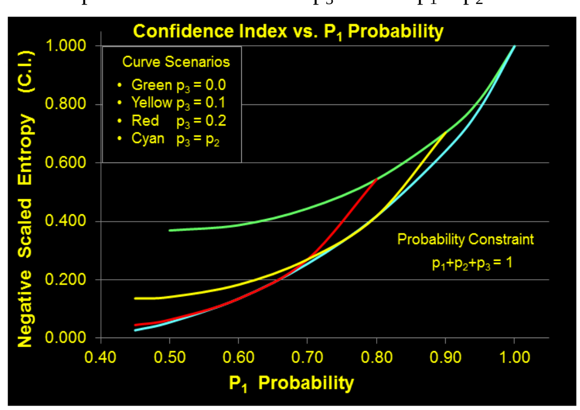

Figure 1: Confidence Index (C.I.) is plotted vs facies probability, p_1, for a three-facies system where p_1, is allowed to vary for various relationships between p2 and p3

10.1190/segam2019-3204859.1

Note the concave nature of the curve, indicating that it is quite sensitive to departures of the winning (highest) probability from unity. The other curves show the effects of various other probability scenarios. In all cases, when the probabilities are increasingly distributed over more facies, the Confidence Index drops.

Example

We demonstrate the above ideas with a Gulf of Mexico data set. The key horizon is the top of the Green sand shown in Figure 2. Sharp discontinuities are the results of faulting. Below the Green horizon, we recognize both upper and lower Green sandstones. Geologically, there is a set of two vertically-stacked deltaic systems of middle Pliocene age. They average about 400 ft. in thickness and are separated by about 500 ft. Within the play area are delta slope deformation, slump-induced turbidites, thin mouth-bed deposits but without the presence of any delta plain facies.

The available seismic consisted of five partial-angle stacks with the maximum angle in the farthest stack being 50 degrees This was not judged to be sufficient to resolve density with any degree of certainty. A single set of wavelets, one for each partial stack, was obtained by matching elastic synthetics to the seismic at each of the seven available wells. The log sets included full-wave sonic logs over the reservoir interval, facilitating the creation of the AVO wavelets. Three facies were identified: Shale, Silty, Pay.

The results of the AVO inversion are shown in Figure 3 with high-cut-filtered logs overlaid. The matches are not perfect since the inversion has no prior knowledge of the high frequency component of the logs. The region of interest is the sand below the black horizon marker where there is the possibility of hydrocarbon deposits. Agreement with the logs is worse in the right of the figure. This is a low frequency effect due to pressure-induced spatial non-stationarities in this band.

The results of the Bayesian facies analysis are shown in Figure 4. Well facies have been overlaid. Agreement with the wells is generally good and the pay has been well defined.

We compared the Confidence Index. for two different facies estimation workflows as described by Pendrel and Schouten, (2018). The first was a Bayesian facies-first approach, the inputs for which were elastic impedances from post-stack inversions. The second procedure used the facies estimation created above and per-facies elastic trends from logs to build a low frequency model for input to a

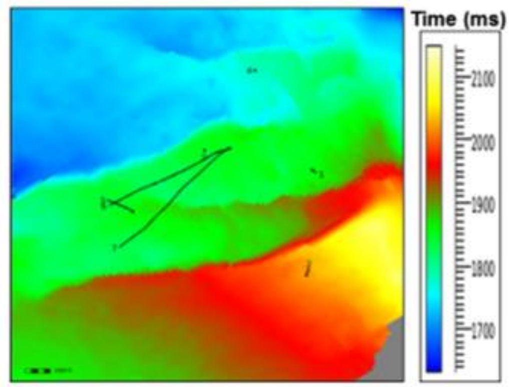

Figure 2: Project map with the upper sand horizon and well locations

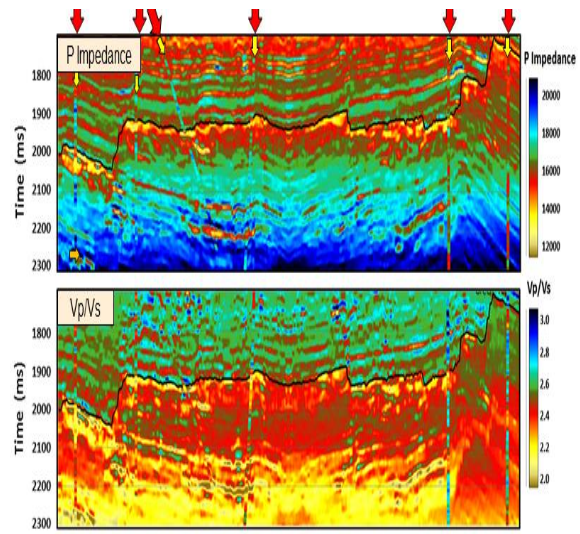

Figure 3: P Impedance (upper) and Vp/Vs (lower) from AVO Inversion. High-cut filtered logs have been overlaid (red arrows). The region of interest is just below the black marker.

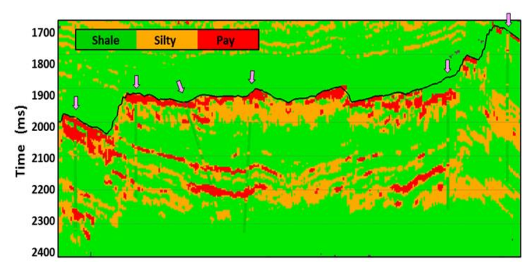

Figure 4: The facies in this figure were determined by applying Bayesian analysis to the P Impedance and Vp/Vs from the AVO inversion. Well facies have been overlaid (pink arrows).

10.1190/segam2019-3204859.1

simultaneous AVO inversion. Facies estimation was then done using the inversion outcomes.

Figure 5 shows the Confidence Index corresponding to the facies probabilities for each workflow. The confidence in the second approach is significantly greater, demonstrating the usefulness of the formal inversion which includes a facies-driven low frequency input model. The facies logs in the plot indicate that the facies-first approach was most successful in delineating Pay. This would be expected since the Pay facies show the most prominent anomalous features in elastic impedances.

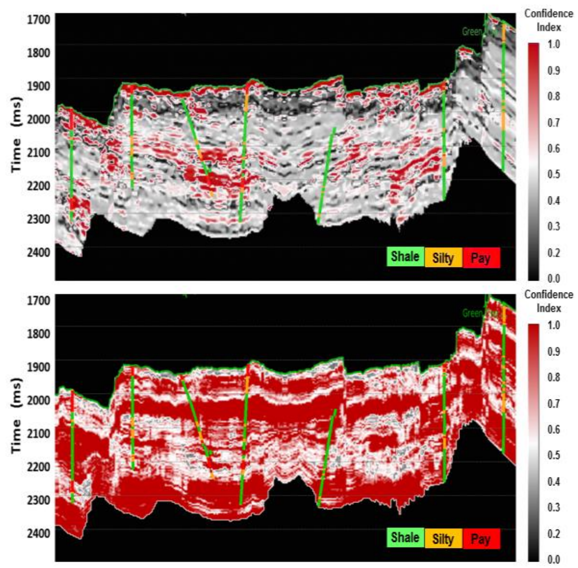

Figure 5: Confidence Index for the facies-first approach (upper) is compared to that for the facies derived from the AVO inversion (lower). Facies logs are overlaid. The AVO inversion method shows significantly larger confidence values.

We have also applied the method to 40 realizations of geostatistical inversion. Each realization consisted of volumes of P Impedance, Vp/Vs and facies, all computed via a simultaneous algorithm. From an analysis of the entire set of realizations, the probabilities of occurrence of each of the three facies were determined. From these, a Confidence Index was computed. The results are shown in Figure 6. The well tracks are readily identifiable, showing high confidence values since they were part of the prior information. Away from the wells, the Confidence Index is reduced in regions of facies transitions. These are regions where two facies show more equal probabilities and could be indicative of the presence of a hybrid facies.

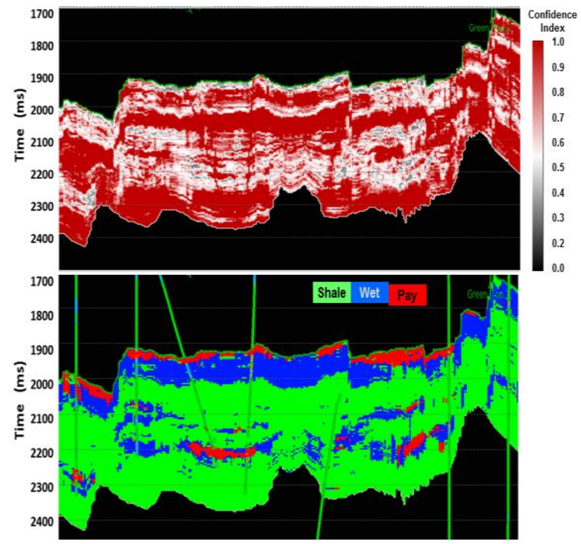

Figure 6: Confidence Index corresponding to facies probabilities from 40 realizations of geostatistical inversion (upper). In the bottom panel are the corresponding facies. Confidence is reduced in regions of facies transitions.

Finally we demonstrate how the notion of Confidence Index can be utilized in the facies design process and the construction of the ePDFs. Figure 7 shows a proposed ePDF design in P Impedance – Vp/Vs space. The first two standard deviations of the proposed ePDFs are shown. The color background is the Confidence Index at each coordinate in the ePDF design space, derived from the proposed PDFs. When facies overlap strongly, the Confidence Index is reduced. It also indicates zero by definition when a point in cross-plot space exceeds a maximum distance threshold from all the PDF means. This is meant to exclude outliers and bad data points. The excluded locations can be mapped and have proved to be useful in identifying new, unforeseen facies. Note that confidence in the intermediate Silty facies is reduced due to its proximity with Shale and Pay.

We estimate uncertainty in P Impedance and Vp/Vs from inversion by comparing high-cut-filtered logs to inversion outcomes at the well locations. These can then be formally included in the Bayesian facies analysis. Their effect is to reduce facies probabilities, making the probabilities of competing facies more similar. The predictable and desired effect on C.I. is a reduction of confidence. Figure 8 shows the effects of including an uncertainty on the Confidence Index. When uncertainty is accounted for, confidence in the overlapping facies regions deteriorates remarkably.

10.1190/segam2019-3204859.1

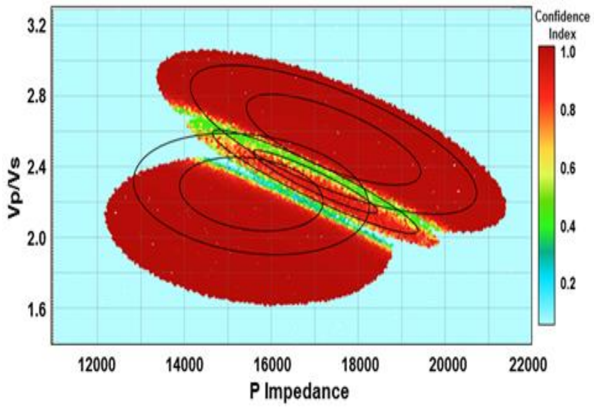

Figure 7: Confidence Index maps corresponding to the proposed elastic PDFs (black) are used to guide the PDF design. There has been no assumed uncertainty in the input inversions.

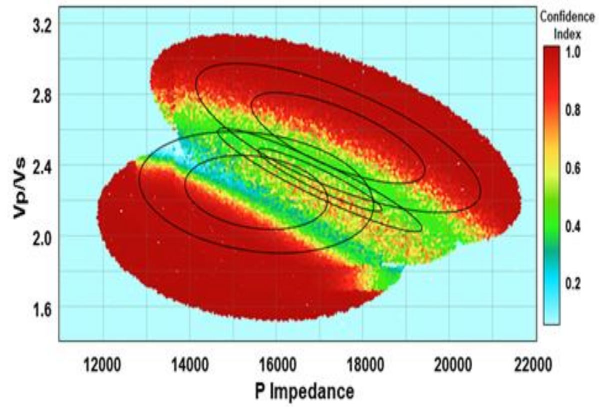

Figure 8: Confidence Index maps corresponding to the proposed elastic PDFs (black). An inversion uncertainty has been included.

Conclusions

We have showed how a Confidence Index based on the concepts of entropy and information theory can be used in various situations to gauge the reliability of Bayesian-derived facies. The method incorporates the probabilities of all the possible facies in a set and provides guidance in judging confidence. We applied the technique to determining the confidence in different inversion workflows and also showed how it could be used to QC the facies from simultaneous geostatistical inversions. Another application to facies PDF design was also demonstrated.

Acknowledgements

The authors wish to thank Stone Energy for permission to show these data. They also thank their colleagues in the CGG GeoSoftware team for their valuable comments and support.

10.1190/segam2019-3204859.1

REFERENCES

Caulfield, C., and J., Curtis, 2018, Seismic information entropy: A new attribute for seismic interpretation: GeoConvention 2018.

Pendrel, J. V., C., Mangat, and M., Feroci, 2006, Using Bayesian inference to compute facies-fluids probabilities: 2006 CSPG-CSEG-CWLS Convention, 278.

Pendrel, J. V., and H. J., Schouten, 2018, A facies-first workflow for the estimation of elastic-reservoir properties: 88th Annual International Meeting, SEG, Expanded Abstracts, 386–390, doi: https://doi.org/10.1190/segam2018-2997902.1.

Pendrel, J. V., and H. J., Schouten, 2019, Confidence measure for Bayesian facies estimations: GeoConvention 2019.

Shannon, C. E., 1948, A mathematical theory of communication: Bell System Technical Journal, **27**, 379–423, doi: https://doi.org/10.1002/j.1538-7305.1948.tb01338.x.